Supplementary Material (supporting Tables and Figures) for manuscript:

The picobirnavirus crystal structure provides functional insights into virion assembly and cell entry

Stéphane Duquerroy[1,2], Bruno Da Costa[3] , Céline Henry[4], Armelle Vigouroux[1,§], Sonia Libersou[5], Jean Lepault[5], Jorge Navaza[5,¶], Bernard Delmas[3] and Félix A. Rey,[1,]*

[1]*Institut Pasteur, Unité de Virologie Structurale, Virology Department and CNRS URA 3015, 75015 Paris, France.*

[2]*Université Paris-Sud, Faculté d'Orsay, 91405 Orsay Cedex, France.*

[3]*INRA UR892, Virologie et Immunologie Moléculaire, 78350 Jouy-en-Josas, France.*

[4]*INRA UR477, Unité BioBac, UR477, 78350 Jouy-en-Josas, France*

[5]*CNRS-INRA UMR 2472, Laboratoire de Virologie Moléculaire et Structurale, Gif-sur-Yvette, France.*

Present addresses: [§] CNRS UPR 3082 LEBS, 91190 Gif-sur-Yvette, France and [¶]CNRS/CEA UMR 5075 IBS, 38027 Grenoble, France.

[*]Correspondence: FAR (rey@pasteur.fr)

Running title: Picobirnavirus crystal structure**.**

Keywords: Double-stranded RNA viruses/gastroenteritis viruses/Structural Virology/Virus crystallography.

Subject Categories: Structural Biology/Microbiology & Pathogens

Correspondence: FAR (rey@pasteur.fr)

Suppl. Table S1: characterization of the local symmetry axes within CP dimers.

Viruses[a]:	**PBV**	**L-A Virus**	**BTV**
RMS deviation (Å)	0.95[*]	1.91	11.84
Rotation Angle (deg.)	179.2	163.6	164.4
Number of Ca atoms	521	651	845
After optimization:			
RMS deviation (Å)	0.81	1.22	1.80
Rotation Angle (deg.)	179.2	163.9	162.7
Number of Ca atoms	516	612	546

[a]The first block lists the RMS deviations and rotation angle calculated for all Cα atoms related by the L2 axis in the corresponding dimer. The second block lists the values obtained after improvement of the transformation by excluding from the superposition all residues outside a cutoff limit of 3.8 Å (Program O).
[*]Imposing a 180° rotation gives to a rms deviation of 0.99 Å for the 521 Cα.

Legends to supplementary Figures

Fig. S1. PBV VLPs purification and analysis.

Top, left panel. Photograph of a representative CsCl gradient tube - visualized by UV light - displaying two bands, at low (LD) and high density (HD), the latter containing most of the material. Middle and left panels: SDS-PAGE analyses of nucleic acid and protein contents, respectively, of the two bands. The nucleic acid markers used in the middle gel correspond to double-stranded DNA fragments obtained by digesting phage Lambda DNA with HindIII and EcoRI. They give a rough idea of mobility, but not the actual molecular weight of the single-stranded RNA molecules of cellular origin contained in the VLPs. In the protein gel (right panel), N-terminal sequencing and mass spectrometry analysis allowed the identification of the two bands indicated in the right (55 and 7 kD, see text).

Bottom: electron micrographs of negatively stained samples of wild type (left) and cleavage site mutant (right) mentioned in the text. The mutant sample gave rise to a single band in the CsCl gradient, with density corresponding to the LD band of wild type. Only a few closed particles are observed; SDS PAGE and N-terminal sequencing confirmed the absence of cleavage.

Fig. S2 : Mass spectrometry analysis of the picobirnavirus 7 kD peptide.

A. MALDI-TOF spectrum of intact VLPs in the mass/charge window ranging from 7,000 to 8,100 Daltons. The left-most peak, at mass/charge (m/z) ratio of 7293.32, represents the signature of the unprocessed peptide [Met1-Asn65]. The five additional major peaks were attributed to acetylations (1 or 2) and oxidations (0, 1 or 2 of the two methionines present in the peptide). Furthermore, the spectrum shows a series of smaller peaks at higher mass/charge values, all equally spaced by 42 Da, compatible with additional acetylations up to the 11 lysine residues present in addition to that at the N-terminus (Note: it is important to bear in

mind that the height of the individual peaks is not proportional to the relative abundance of the corresponding molecule). The then vertical black lines are separated by 42 Daltons (also indicated by the double arrow), to highlight the periodicity. The numbers next to the short and long lines indicate the number of acteyl groups added to the peptide having one or two oxidated methionines, respectively. A "*" symbol indicates the modified peptide that was ascertained to possess an acetylated N-terminus and an oxidized initiation methionine. These two peptide modifications were identified by electron transfer dissociation (ETD, LTQ-ETD Thermo Fisher Scientific) mass spectrometry analysis of the peptide digested by chymotrypsin. The resulting sub-peptide was identified as Acetyl-MoxKKESSKSFPKSH, Mere Mox indicates the oxidized Met residue. "**" symbol: the monoisotopic neutral mass of this peptide was measured by Fourier-transform ion cyclotron resonance (FTICR-MS APEX III, Brucker Daltonics, Bremen, Germany) mass spectrometry to be 7389.5696. This mass is in agreement with the theoretical mass of the peptide with two acetylations and one oxidation, which is 7389.5603. The high precision of this measurement was necessary to rule out the presence of a myristoyl group in the peptide.

B. Comparison of the theoretical and experimental average masses of the peptides in the major peaks of the MALDI-TOF spectrum. Stars indicate the two peptides ascertained by ETD and FTICR mass spectrometry.

METHODS: 10µl of the purified VLP suspension were desalted on ZipTip C18 (Millipore) and eluted with 0.5 µl of 70% (vol/vol) acetonitrile–0.3% (vol/vol) trifluoroacetic acid. The eluate was directly spotted onto the MALDI plate. 1µl of 2,5-dihydroxybenzoic acid at a concentration of 10 mg/ml in 50% (vol/vol) acetonitrile–0.1% (vol/vol) trifluororacetic acid was loaded on the sample. Mixing the suspensions was carried out directly onto the MALDI plate and the suspension was dried at room temperature. Shoots were directed on needle crystal. Mass spectra were acquired on a Voyager-DE-STR time-of-

flight mass spectrometer (Applied Biosystems, Framingham, Mass.) equipped with a nitrogen laser emitting at λ= 337 nm (Laser Science, Franklin, Massachusetts). The accelerating voltage used was 25 kV. All spectra were recorded in the positive linear mode with a delayed extraction of 800 ns and a 94 % grid voltage. Calibration was done using bovine insulin (M + H)+ = 5734.6 Da and cytochrome C (M + H)+ = 12361.1 Da.

Fig. S3 : Purified PBV particles disrupt liposomes *in vitro.*

Kinetics of the release of encapsulated 6-carboxyfluorescein (CF) from unilamellar liposomes induced by purified PBV particles. Addition of a PVB particle suspension (final protein concentration of 0.18 μg/ml) to the liposomes induces significant time-dependent increase of CF fluorescence from PC liposomes and a destabilization of the liposome membrane (yellow curve) contrary to addition of the plain buffer (purple curve). Trypsin proteolysis increases the membrane destabilization activity of PBV particles (red curve). Note that trypsin has no effect on liposomes (blue curve).

METHODS. Phosphatidyl choline (PC) and CF were purchased from Sigma. Dried lipids (100 μg) obtained after removal of the solvent (1:1 ethanol-chloroform mixture) were suspended in LTN buffer (15 mM NaCl, 5 mM Tris pH 8.0). A concentrated solution of CF was added to the lipid suspension (final concentration 50 mM). The suspension was vortexed for one minute and frozen and thawed three times using liquid nitrogen. Finally the liposome suspension was sonicated for 15 minutes in a Branson 2510 bath sonicator. Liposomes encapsulating CF were separated from free CF by eluting the mixture through small Sephadex G200 columns equilibrated with 50 mM NaCl, 50 mM Tris pH 8.0. The release of CF was monitored by the increase of fluorescence at 516nm, using a 492nm exciting band in a Perkin Elmer LS50B spectrofluorimeter fitted with a circulating bath to maintain the temperature at 37°C. The value of 100% release of the encapsulated dye was obtained by the addition of Triton X-100 at the end of the reaction. The percentage of CF release induced by the PBV

particles was calculated as: 100(F-F0)/(FT-F0) were F is the measured fluorescence FT is the fluorescence after addition of Triton and F0 the initial fluorescence.

Fig. S4. Quality of the experimental electron density and stereo diagram of the alpha-carbon trace.

A and B. Stereo diagram showing the experimental electron density map (A) and the final sigmaa-weighted 2Fo-Fc map (B) displayed as mesh contoured at 1 standard deviation of the map and superposed to the refined atomic model, displayed as sticks colored according to atom type (green, red and blue for carbon, oxygen and nitrogen, respectively). The region of the model corresponds to residues 290-320 (β8-α8 region in Fig. 1A). The grid size of the electron density mesh is 0.88 Å in A and 0.62 Å in B.

C. Stereo view of the alpha-carbon trace of one subunit in the CP dimer.

Fig. S5. The CP dimer is essentially 2-fold symmetric.

The Figure shows a superposition of the two polypeptide chains of the CP dimer, in blue and grey (colored as in Fig. 4). There are only minor deviations from 2-fold symmetry, except for a different conformation of the very C-terminal residues, which are ordered only in the subunit that reaches the I5 axis (subunit A, in blue, the extended segment spanning residues 587 to 590 is clearly visible in Fig. 3A, right panel). Icosahedral axes I2, I3* (the * and red color is to highlight that it was transformed by the L2 operation) and I5, and the L2 axis are drawn and labeled. Side chains of residues Asn A157 and Asn B221, located at the I5 and I3 axes, respectively, and discussed in the text, are represented as colored ball and stick. Labeled are residues 283-285, 392, 582 and C-ter, where maximal displacements are observed, and which were removed in the optimization of the L2 operation provided in suppl. Table S1.

Fig. S6. Hydrogen-bonding network surrounding the trans-proteolytically processed N-terminus of CP.

The main chains subunits A and B are displayed as blue and grey ribbons, respectively (i.e., colored as in Fig.2, and labeled according to Fig. 1). The side chains of selected residues are displayed as ball and stick, colored by atom: nitrogen, blue; oxygen, red; carbon, white or grey, for chains A or B, respectively. Broken lines denote hydrogen bonds. The pink sphere indicates a bound water molecule, found in both independent subunits. The side chain of Asp 66 points to solvent at the interior of the particle.

Suppl. Fig. S1

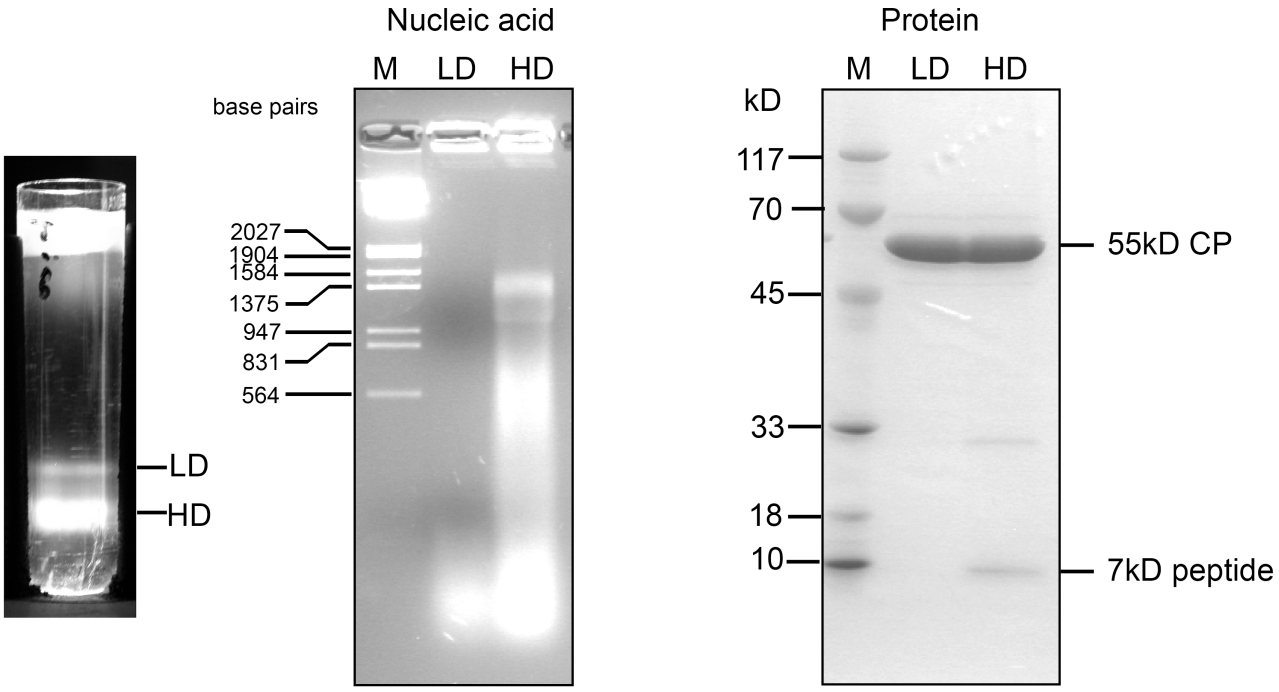

wild type:

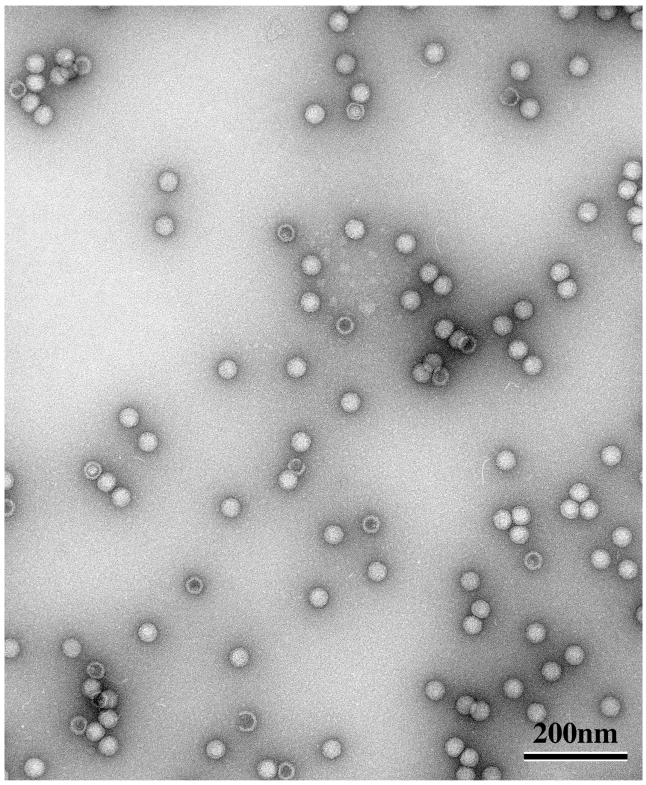

N65E,D66F double mutant:

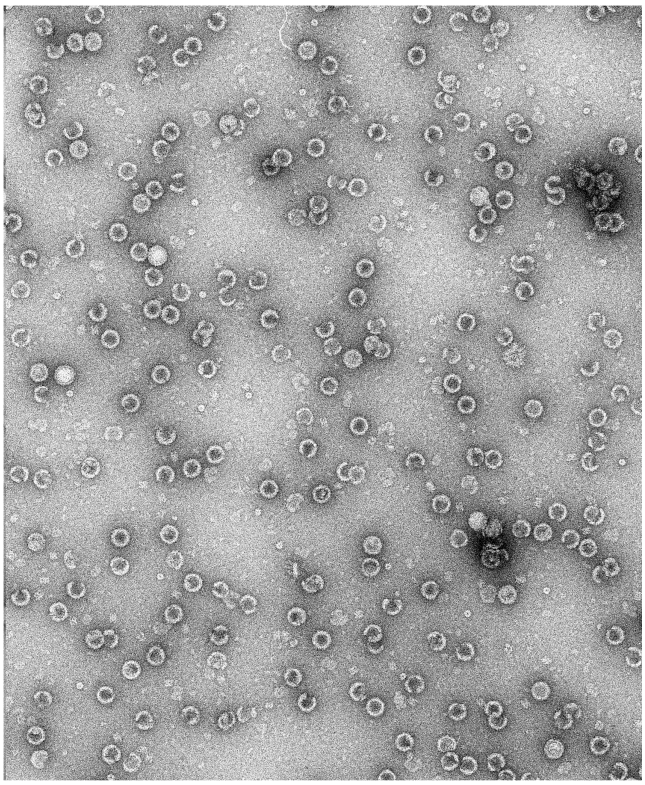

Suppl. Fig. S2

A.

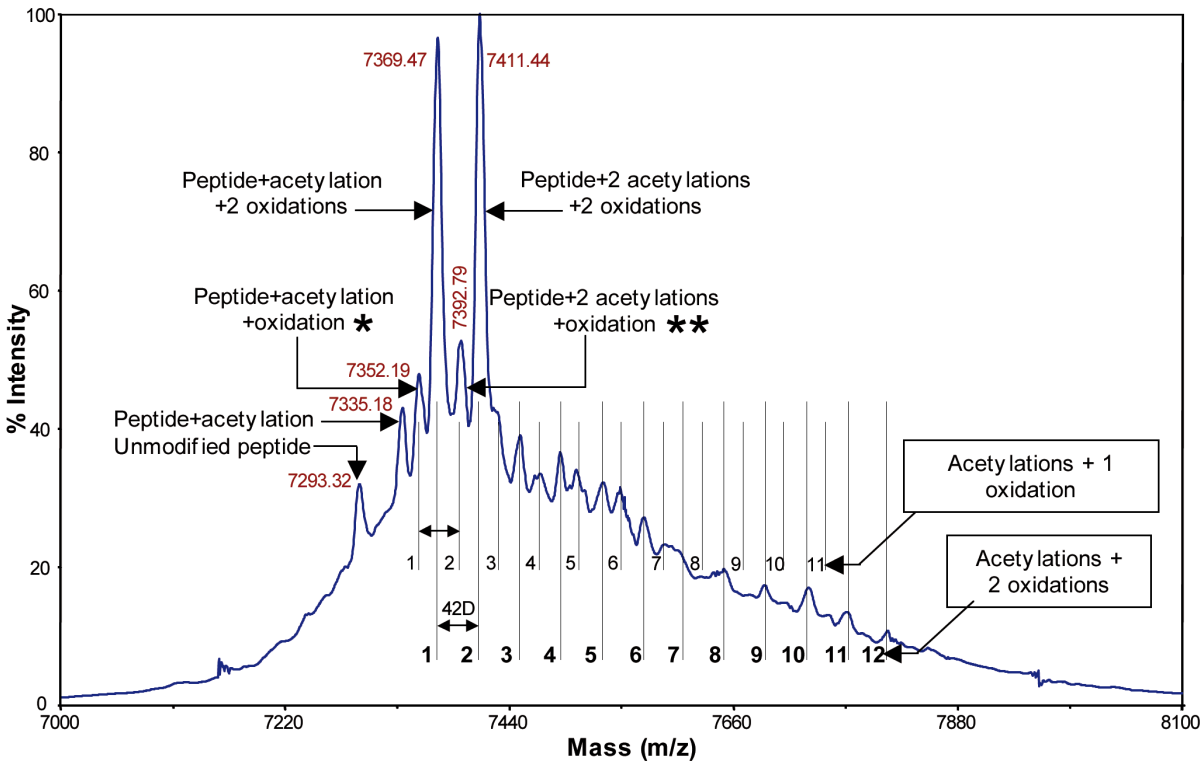

B.

	(M+H)+ theoretical average mass	(M+H)+ experimental average mass
Peptide	7295,08	7293,32
Peptide+acetylation	7337,12	7335,18
Peptide+acetylation+oxydation*	7353,12	7352,19
Peptide+acetylation+2 oxydations	7369,12	7369,47
Peptide+2 acetylations+oxydation**	7395,16	7392,79
Peptide+2 acetylations+2 oxydations	7411,16	7411,44

Suppl. Fig. S3

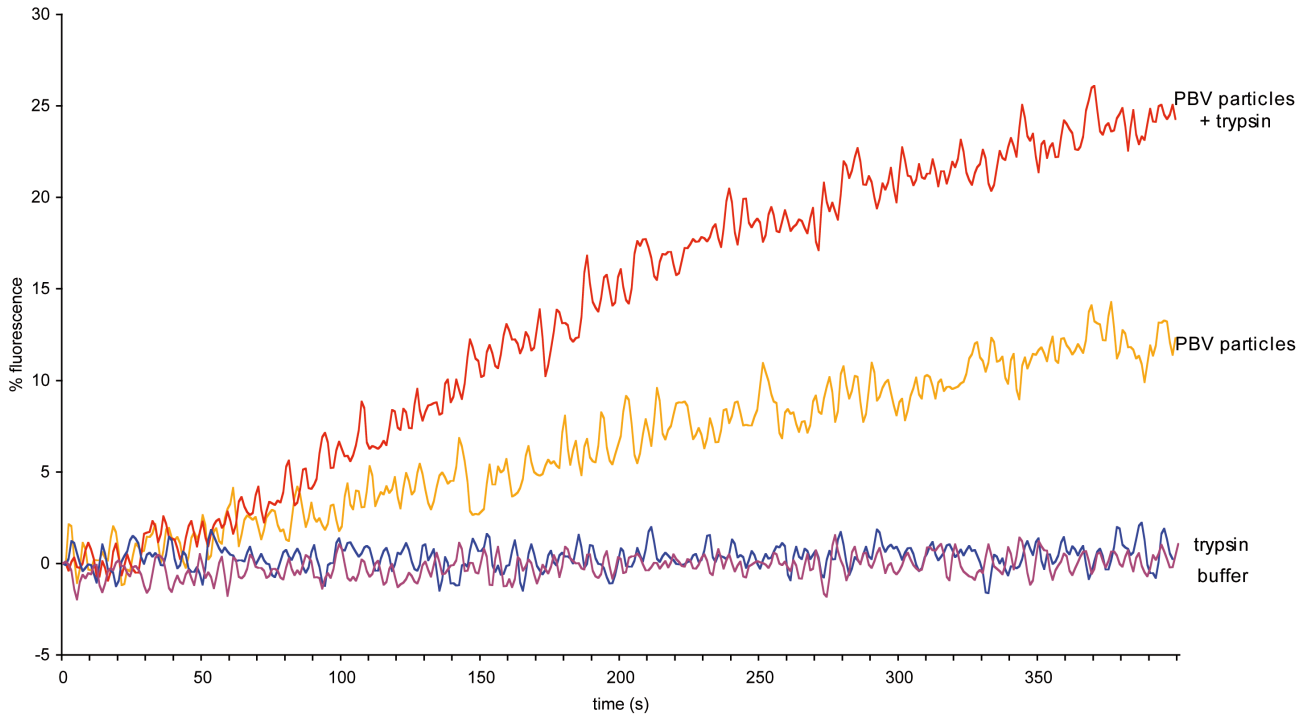
30
25
20
15
10
5
0
-5
% fluorescence
0
50
100
150
200
250
300
350
time (s)
PBV particles
+ trypsin
PBV particles
trypsin
buffer

Suppl. Fig. S4

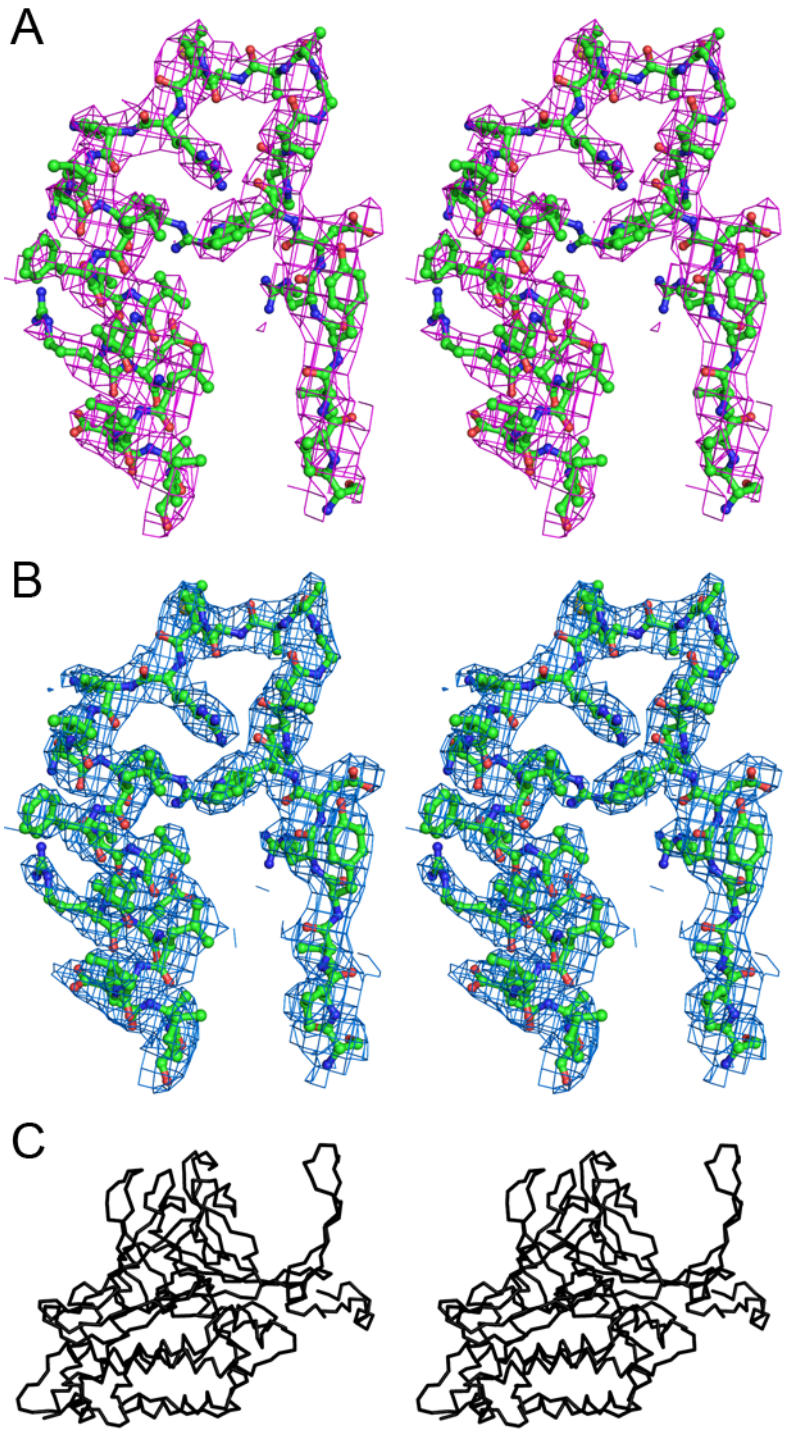

Suppl. Fig. S5

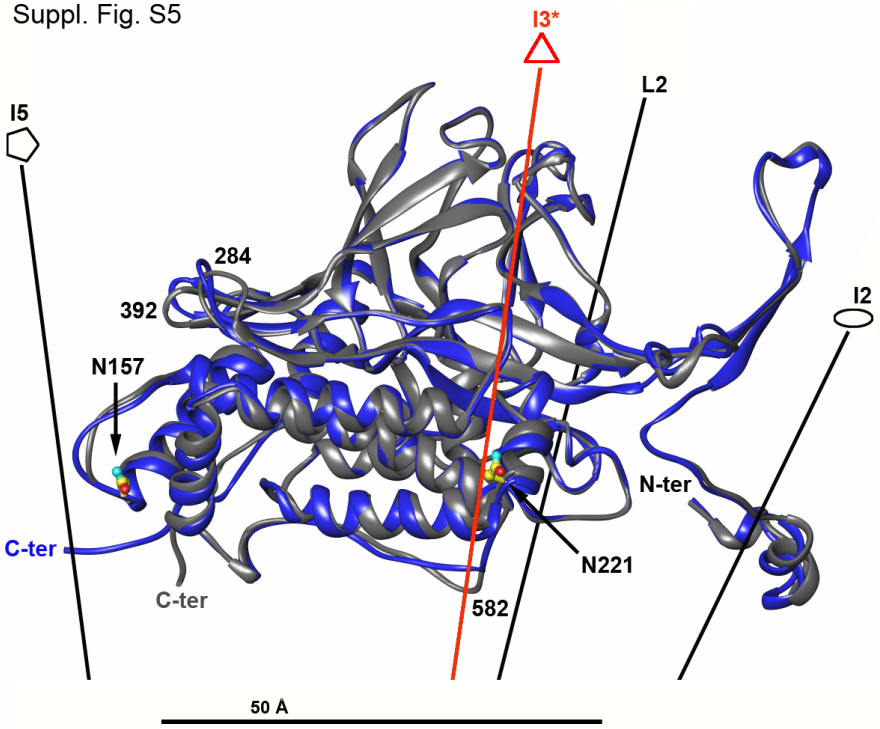

Suppl. Fig. S6

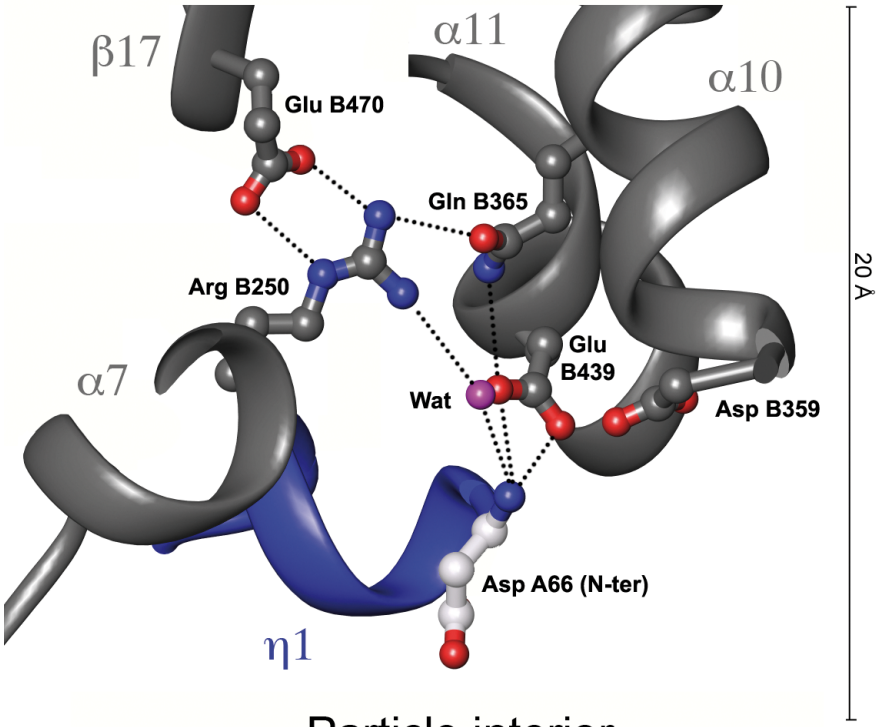

Particle interior